Identification, expression analysis and molecular modeling of *Iron deficiency specific clone 3* (*Ids3*) like gene in hexaploid wheat

Priyanka Mathpal[1†], Upendra Kumar[2†] Anuj Kumar[3], Sanjay Kumar[4], Sachin Malik[1], Naveen Kumar[1], H. S. Dhaliwal[5], Sundip Kumar[1]*

[1]Molecular Cytogenetics Laboratory, Molecular Biology & Genetic Engineering, College of Basic Sciences & Humanities, GB Pant University of Agriculture & Technology, Pantnagar-263145, Uttarakhand, India

[2]Department of Botany & Plant Physiology, College of Basic Sciences & Humanities, Ch. Charan Singh Haryana Agricultural University, Hisar-125004 Haryana India.

[3]Advanced Centre for Computational & Applied Biotechnology, Uttarakhand Council for Biotechnology, Dehradun-248007, Uttarakhand, India

[4]Centre for Bioinformatics, Biotech Park, Lucknow-226021, Uttar Pradesh, India

[5]Akal School of Biotechnology, Eternal University, Baru Sahib, Himachal Pradesh, India

* Corresponding Author

Email: malik.sundip@gmail.com

[†]These authors contributed equally to this work.

Abstract

Graminaceous plants secrete iron (Fe) chelators called mugineic acid family phytosiderophores (MAs) from their roots for solubilisation and mobilization of unavailable ferric (Fe^{3+}) ions from the soil. The hydroxylated forms of these phytosiderophores have been found more efficient in chelation and subsequent uptake of minerals from soil which are available in very small quantities. The genes responsible for hydroxylation of phytosiderophores have been recognized as iron deficiency-specific clone 2 (*Ids2*) and iron deficiency-specific clone 3 (*Ids3*) in barley but their presence is not reported earlier in hexaploid wheat. Hence, the present investigation was done with the aim:(i) to search for the putative *Hordeum vulgare Ids3* (*HvIds3*) ortholog in hexaploid wheat, (ii) physical mapping of *HvIds3* ortholog on wheat chromosome using cytogenetic stocks developed in the background of wheat cultivar Chinese Spring and (iii) to analyze the effect of iron starvation on the expression pattern of this ortholog at transcription level. In the present investigation, a putative ortholog of *HvIds3* gene was identified in hexaploid wheat using different bioinformatics tools. Further, protein structure of TaIDS3 was modelled using homology modeling and also evaluated modelled structure behavior on nanoseconds using molecular dynamics based approach. Additionally, the ProFunc results also predict the functional

similarity between the proteins of *HvIds3* and its wheat ortholog (*TaIds3*). The physical mapping study with the use of cytogenetic stocks confines *TaIds3* in the telomeric region of chromosome 7AS which supports the results obtained by bioinformatics analysis. The relative expression analysis of *TaIds3* indicated that the detectable expression of *TaIds3* induces after 5th day of Fe-starvation and increases gradually up to 15th day and thereafter decreases till 35th day of Fe-starvation. This reflects that Fe deficiency directly regulates the induction of *TaIds3* in the roots of hexaploid wheat.

Keywords

Phytosiderophores, *Ids3*, Hexaploid wheat, Physical mapping, Fe-deficient

Introduction

Iron (Fe) deficiency, a major abiotic stress, especially in calcareous soils (~30% of the world's cultivated soils) with extremely low solubility of Fe (owing to high pH levels) reduces crop yield. The low availability of Fe results into its poor uptake by plants, which causes severe yield losses. Further, the poor uptake of other minerals by plants also reduces the overall mineral content in grains, which are essential to meet the required human dietary needs (Cakmak 2008).

The manifestation of Fe deficiency in calcareous soils has been recognised as Fe-chlorosis and lime-induced chlorosis. Under adverse conditions of Fe deficiency, graminaceous plants secrete Fe-chelators called mugineic acid family phytosiderophores from their roots (Takagi 1978). Mugineic acid family phytosiderophores (MAs) are highly effective in solubilisation and mobilization of Fe in calcareous soil (Treeby et al. 1989) and are involved in the uptake of Fe through roots (Romeheld and Marschner 1990; vonWiren et al. 1995) to acquire sparingly soluble Fe as Fe^{3+}-MAs complex through the use of Fe^{3+}-MA transporters. The secretion of MAs increase under deficiency of Fe and is correlated with plant's tolerance to Fe deficiency. The quantity and different forms of phytosiderophores secreted by roots play an important role in providing tolerance to plants in Fe-deficient condition. The hydroxylated forms of phytosiderophores like 3-hydroxymugineic acid (HMA) and 3-epihydroxymugineic acid (epiHMA) have been found more efficient in chelation and subsequent uptake of trace minerals (vonWiren et al. 2000). In *Hordeum vulgare*, the genes responsible for hydroxylation of phytosiderophores have been recognized as *iron deficiency-specific clone 2* (*Ids2*) and *iron deficiency-specific clone 3* (*Ids3*) (Nakanishi et al. 2000). The *Ids3* gene encodes an enzyme dioxygenase which hydroxylates the C-2' position of 2'-deoxymugineic acid (DMA) and 3-epihydroxy-2'-deoxymugineic acid

(epiHDMA) and converts DMA to MA or epiHDMA to epiHMA, while *Ids2* hydroxylates C-3' position of MA and DMA and converts MA to epiHMA or DMA to epiHDMA. MA, epiHDMA and epiHMA are more stable under mildly acidic conditions and might be more favourable for inter mineral translocation (Kobayashi and Nishizawa 2012). As reported in publicly available sequence databases, *Ids2* is having 3,411 bp long coding sequence which encodes a protein of 338 amino acids (http://www.uniprot.org/uniprot/Q40061) while *Ids3* have 4,904 bp long coding sequence which encodes a protein of 339 amino acids (http://www.uniprot.org/uniprot/Q40062). The expression of *Ids3* is always much stronger than that of *Ids2* in Fe-deficient condition, indicating that initially DMA changes into MA predominantly (Nakanishi et al. 2000).

The biosynthetic pathway for mugineic acid production is well documented in graminaceous crops (Ma and Nomoto 1993). All MAs share the pathway from methionine to DMA and the DMA is then converted to other MAs like HMA, epiHMA and epiHDMA. The pathway up to DMA synthesis is conserved in all graminaceous plants and the variation is in the type of phytosiderophores synthesized in the further hydroxylation steps (Takahashi 2003). It is reported that wheat cultivar Chinese Spring used in the present study produces only one phytosiderophore, namely DMA (non-hydroxylated form) whereas barley cv. Betzes and rye each synthesizes four types of MAs i.e. DMA, MA, epi-HDMA and epi-HMA (Nakanishi et al. 2000; Mori et al. 1990; Neelam et al. 2011). It has been reported that wheat and its wild progenitors do not have the ability to secrete MA and HMA from the beginning of their evolution because they lack the ability to secrete MA and HMA as a result of the absence of IDS3 enzyme (Singh et al. 1973). Therefore, no efforts were made in the past to study *Ids3* gene in wheat genome.

In view of the above, the present investigation was aimed at the identification and physical mapping of the wheat ortholog of *Ids3* gene and to analyze its expression pattern under Fe-deficient conditions in hexaploid wheat.

Materials and Methods

Plant Growth Conditions

Seeds of wheat cultivar Chinese Spring were surface sterilized and soaked on filter paper with distilled water and incubated in dark at 25 °C until germination. Then the three-days old seedlings were transplanted and cultured hydroponically in 2.0 litre plastic boxes with continuous air flow under Fe-sufficient (+Fe) and Fe-deficient (-Fe) conditions. The 1X concentration of the nutrient solution for hydroponic culture consisted of 2.0mM $Ca(NO_3)_2$, 0.7mM K_2SO_4, 0.1mM KCl, 0.1mM KH_2PO_4, 0.50mM $MgSO_4$, 0.15mM Fe^{3+}-EDTA, 10µM

H_3BO_3, 0.5µM $MnSO_4$, 0.5µM $ZnSO_4$, 0.2µM $CuSO_4$ and 0.01µM $(NH_4)_6Mo_7O_{24}$. The nutrient solution was replaced once per week and its pH adjusted to 5.5 to 5.6 daily with 1N HCL. For expression study under Fe starvation, wheat cultivar Chinese Spring was grown at 23-25 °C under a 16/8 h light (~160 µmol/m^2.s)/dark regimen.

Identification of *Hordeum vulgare Ids3* homolog through *in-silico* approach

In-silico analysis was performed to identify the putative ortholog(s) of *HvIds3* gene in hexaploid wheat. Full length genomic sequence of *HvIds3* gene (Accession Number AB024058.1) was retrieved from NCBI (National Center of the Biotechnology Information) (http://www.ncbi.nlm.nih.gov/) in FASTA format. Similarity searches were carried out using genomic sequence of *HvIds3* as a query against the wheat chromosome survey sequences available athttp://urgi.versailles.inra.fr/using the BLAST (Basic Local Alignment Search Tool) search engine (http://www.ncbi.nlm.gov/BLAST). The matching wheat contigs having good coverage (>85%), identity (>70%) and e-value (<e-10) were downloaded. The exon/intron structure prediction in the selected wheat contigs was carried out using FGENESH+ (http://linux1.softberry.com/berry.phtml) program. Conserved domain search (CD-Search) program was used to predict functional domain(s) in the sequences of *HvIds3* and its wheat ortholog *TaIds3* (http://www.ncbi.nlm.nih.gov/Structure/cdd/cdd.shtml).

Multiple sequence alignment (MSA) between *HvIds3* and three copies of *TaIds3* (*TaIds3*_7AS, *TaIds3*_7BS, and *TaIds3*_7DS) was performed by using CLUSTAL W2 (www.ebi.ac.uk/Tools/msa/clustalw2) available on EMBL-EBI (www.ebi.ac.uk). The 3D structure of proteins (*HvIds3* and *TaIds3*) was predicted using homology modeling based Swiss-Model server (http://swissmodel.expasy.org/). Flexible structure AlignmenT by Chaining AFPs (Aligned Fragment Pairs) with Twists (FATCAT) structure alignment tool (http://fatcat.burnham.org/) was used for the alignment of 3D structure model of proteins. ProFunc (http://www.ebi.ac.uk/thornton-srv/databases/ProFunc/) was used to predict the biochemical function of *TaIds3* based on the predicted 3D model. Sub cellular localization of *HvIds3* and *TaIds3* was predicted with TargetP 1.1 (http://www.cbs.dtu.dk/services/TargetP/) and PLANT-mPLoc (http://www.csbio.sjtu.edu.cn/cgi-bin/PlantmPLoc.cgi), respectively.

Cytogenetic Stocks

To facilitate the mapping of wheat ortholog of *Ids3* gene to the individual chromosome, chromosome arm and sub chromosomal location (i.e. deletion bin), the following cytogeneticstocks in the background of wheat cultivar Chinese Spring were used: (i) 22 nullisomic-tetrasomic (NT) lines (Sears 1954; Sears1964) (ii) two ditelosomic (Dt)

lines i.e. 7AS and 7AL (Sears and Sears 1978) and (iii) 8 homozygous deletion (Del) lines of chromosome 7AS (Endo and Gill 1996). Seeds of NT, Dt and Del lines were procured from the Wheat Genetic and Genomic Resources Center at the Kansas State University, Manhattan, USA and multiplied in the greenhouse facility at the G. B. Pant University of Agriculture & Technology at Pantnagar, India.

DNA isolation and primer designing

The genomic DNA from fresh leaves of cytogenetic stocks and wheat cultivar Chinese Spring was extracted using CTAB (Cetyltrimethyl ammonium bromide) method with some modifications (Maroof et al. 1994). To confirm the chromosomal location of *TaIds3,* a pair of 7AS chromosome specific primer was designed using primer blast software (http://www.ncbi.nlm.nih.gov/tools/primer-blast/) (Table 1).

Polymerase Chain Reaction

Polymerase chain reaction (PCR) amplification was carried out in a volume of 20 µl in Applied Biosystems (Veriti 96 well) thermal cycler. The reaction mixture contained 80-100 ng of template DNA, 1X PCR buffer, 1.5mM $MgCl_2$, 0.25mMdNTP, 500nM of each PCR primer (forward and reverse) and 1.0 U *Taq* DNA polymerase (New England Biolabs). PCR cycling conditions were as follows: 95 °C for 2.30 min followed by 35 cycles of 95 °C for 50 s, 56°C for 40 s and 68 °C for 1.0 min with a final extension of 68°C for 5 min. The PCR products were resolved using 10% polyacrylamide gel electrophoresis (PAGE) and visualized with silver staining (Tegelstrom 1992).

RNA extraction and real time reverse-transcription PCR (RT-PCR) analysis

100 mg root samples were harvested at 5, 10, 15, 25 and 35 days after the plants were exposed to +Fe and –Fe conditions and used immediately for RNA isolation. Root tissues were frozen in 2 ml micro centrifuge tubes and disrupted under frozen conditions using two stainless steel beads (5 mm diameter) in the Tissuelyser (Qiagen, USA). Total RNA was extracted from the disrupted tissue using the GeneJET Plant RNA purification kit (Fermentas Life Sciences) according to the manufacturer's protocol in duplicates. The quantity and quality of the total RNA were evaluated using a nanophotometer (Nanodrop 1000, Thermo-scientific) and visualized by 1% agarose gel electrophoresis. Approximately 1 µg of total RNA was reverse transcribed to cDNA in 20 µL reaction using oligo-dT and M-MLV reverse transcriptase (Fermentas Life Sciences). Real-time PCR primer was designed to amplify a 100–200 bp fragment in untranslated regions. The primer was designed from the conserved region of mRNA of all predicted TaIds3 orthologs using Primer Express® Software version 3.0 (Applied Biosystems) (Table 2).

Real-time RT-PCR was performed with a Step One Plus Real-Time PCR System using SYBR Select Master Mix (Applied Biosystems, USA). Reactions were performed in a total volume of 10 µL with 0.2µM of each primer, 1× SYBR premix, 50ng cDNA and ddH_2O. Reactions were cycled under the following conditions: initial denaturation at 95°C for 2 min, followed by 40 cycles composed of 15 seconds denaturation at 95°C and 1.0 min of annealing/extension at 60 °C. To verify specific amplification, melting curve analysis was performed at 65 °C to 95 °C with the fluorescence continuously being monitored. Data were analysed via $2^{-\Delta\Delta C}{}_T$ method with the v2.3 Software (Applied Biosystems, USA) (Livak and Schmittgen, 2001) and the expression level of housekeeping gene *TaADP* ribosylation factor was used as an internal control (Poalacci et al. 2009) (Table 1). For all real-time PCR analysis, two biological replicates were used and three technical replicates were performed for each biological replicate.

Molecular Dynamics simulations

Molecular dynamics (MD) simulations have become one of the most important techniques in biophysics and helpful to understanding the behaviour of biological macromolecules on nanosecond to microsecond time scales (Gajula et al. 2017). To check the stability of modelled structure of IDS3, we performed molecular dynamics (MD) simulation carried out by Desmond v3.6 (Shiva Kumar et al. 2010; Guo Z et al. 2010; Kevin et al. 2006) implemented in Schrodinger-maestro2017 (Schrödinger Release 2017-2). Protein model preparation done by assigning bond orders, hydrogen atoms added in protein model with neutral pH 7.0 applied by PROPKA (Hui et al. 2005) method. Total 5307 TIP3P (Jorgensen et al. 1983) water solvent atoms were added in truncated octahedron simulation box under periodic boundary conditions and shape and size was set at 10.0Å buffered distance. To neutralize the simulation system electrically, added Na+/Cl- ions to stabilize box charge and were place to randomly in the solvated system. After preparing simulation box (Box size=19882) was proceed to energy minimization by applied 800 steps of steepest descent algorithm followed 2000 steps of conjugate gradient algorithm with 120.0 kcal/mol/Å convergence threshold energy under NPT ensemble. The 300K temperature was applied using Nose-Hoover (Nosé, 1984; Hoover and William, 1984) chain method and 1 atmospheric pressure applied by Martyna-Tobias-Klein (MTK) (Martyna et al. 1994) Barostat method. For both ensemble classes (NPT and NVT) OPLS2005 (Jorgensen et

al.1996; Kaminski et al. 2001) force field were used. Finally, simulation system was set in relaxation state and run for 20nsec.Trajectory recorded in each 4.8psec.

Simulation Trajectory analysis

The 20 nsec MD simulation trajectory was analyses by simulation event and interaction diagram program module available in Desmond v3.6. For protein stability analysis we select root-mean-square deviation (RMSD) value and root mean square fluctuation (RMSF) selected for determination of fluctuation/thermal motion in protein residues during simulation. We analyze the protein contribution of secondary structure elements (SSE) during simulation in structure stabilization.

Results

In-silico mapping and functional annotation

Putative wheat ortholog of *HvIds3* gene was identified using different bioinformatics based algorithms. The results suggested the presence of 2OG-FeII Oxy domain (Pfam Id-CL0029) belonging to DIOX protein family (Fig. S1) in wheat ortholog of *HvIds3*.Further, *HvIds3* sequence was aligned against wheat survey sequences available on IWGSC database. BLASTN results showed 74% sequence similarity with IWGSC_chr7AS_ab_k71 contig of chromosome 7AS, 88% sequence similarity with IWGSC_chr7BS_ab_k71 contig of chromosome 7BS and 78% with IWGSC_chr7DS_ab_k71 contig of chromosome 7DS in wheat genome. The predicted structure of 7AS and 7BS contained 4 exons and the structure belonging to 7DS contained 3 exons. *TaIds3_7AS* and *TaIds3_7BS* coded for 339 and 309 amino acid long protein respectively, while *TaIds3_7DS* coded 242 amino acids length protein which was comparable to the protein of the known gene *HvIds3* of barley. Further MSA results predicted by CLUSTALW2 revealed that *TaIds3_7AS* shared high similarity with *HvIds3* as compared to *TaIds3_7BS* and *TaIds3_7DS* (Fig. S2).With the aim to confirm the chromosomal location of *TaIds3* in hexaploid wheat genome, when contig IWGSC_chr7AS_ab_k71 was used to BLAST against *Triticum aestivum* DNA database in Ensembl plants database, it gave a hit on telomeric region of 7AS.

Out of three predicted wheat orthologs, only *TaIds3* on 7AS had complete gene structure (Fig. 1A).. Transcription start site (TSS) for *TaIds3* on 7BS and 7DS could not be predicted. CD search for these predicted genes showed that *TaIds3_7AS* with 2OG-FeII Oxy domain belonging to DIOX protein family similar to the gene *HvIds3*, while this domain was not fully present in *TaIds3_7BS* and *TaIds3_7DS* (Fig. 1B).

Protein Structure Modeling and Phylogeny Analysis

Swiss-Model software (homology based algorithm) was used to generate 3D model wheat proteins encoded by *Ids3* gene based on 1w9yA template from the Protein Data Bank (PDB) at Root Mean Square Deviation (RMSD) 2.0. UCSF-CHIMERA visualized the different chemical shapes of modelled *TaIDS3* (Fig. 1C). The alignment of the structure of the proteins encoded by *HvIds3* and *TaIds3_7AS* using FATCAT superposition showed 57.25% similarity between the *HvIds3* and *TaIds3* proteins (Fig.S3). ProFunc server was used to determine the biochemical function of *Ids3* in wheat showing catalytic activity (59.07) and oxidoreductase activity (49.52) (Table 1). To identify the sub cellular localization of *TaIds3* using machine-learning program PLANT-mPLoc suggests the cytoplasmic localization of *HvIds3*, *TaIds3_7AS*, *TaIds3_7BS*, and *TaIds3_7DS*, (Table 2).

The phylogenetic tree generated the individual branches for *TaIds3*, *HvIds3*, *HvIds2*, and *OsIds2* (Fig.2). *TaIds3* gene clusters shared the close evolutionary relationship with *HvIds3*, while *OsIds2* and *OsIds3* shared the relationship with *HvIds2*.

Physical mapping of *TaIds3* on 7AS chromosome

In order to confirm the chromosomal location of *TaIds3* in hexaploid wheat genome, the genomic DNA of the cytogenetic stocks developed in Chinese Spring wheat background, was amplified with a pair of 7AS specific primers of *TaIds3* gene. The PCR products of 22 NT lines and di-telocentric lines of 7A are illustrated in Figure 3. The PAGE analysis of the PCR products resolved that a single fragment of *TaIds3* was amplified in 20NT lines, while there was no amplification in N7A-T7B and N7A-T7D. The amplification of the fragment in all 20 NT lines and absence in N7A-T7B and N7A-T7D indicates the presence of this fragment on chromosome 7A (Fig.4). Further, to localize the fragment on the specific arm of 7A chromosome, the genomic DNA of Dt7AS and Dt7AL was amplified with the same primers. The PAGE analysis of the PCR product resolved that there was no amplification in Dt7AL while Dt7AS line gave the amplification with 7AS specific primers (Fig. 3). These results indicate the location of the gene on short arm of 7A chromosome. Further, the genomic DNA of deletion lines of 7AS didn't give any amplification. Therefore, it was confirmed that *TaIds3* is located in the telomeric region of 7AS. On the basis of the above results, the location of *TaIds3* gene is illustrated in Fig.4.

Expression analysis under Fe-starvation

The results of Real-time RT-PCR showed that the detectable expression of *TaIds3* was started on 5thday (2.5 fold) after Fe-starvation. In response to Fe-deficiency, the relative expression was increased gradually up to 15thday (maximum33.5 fold) afterwards decreased in 25thand 35thdays analysis. However, in Fe-sufficient condition, the expressionof *TaIds3* was detectable but almost constant at all stages (Fig.5). The relative expression analysis reflected that Fe deficiency directly regulates the induction of *TaIds3* expression in Chinese Spring roots. The expression of *TaIds3* in Fe-deficient roots was much greater than Fe-sufficient roots at all stages (Fig.5).

Molecular dynamics simulations

The molecular dynamics simulation concerned with stability and fluctuations in protein model of ids3 by analyzing 20nsec simulation trajectories. RMSD plot in Fig. 6B is show protein structure has RMSD between 1.3Å – 2.7Å. From the starting point (1nsec) of simulation, RMSD shows higher value between 3.4Å – 3.7Å, because protein structure has large loop region residues 4-46 that's why it shows conformational changes between 1 to 3nsec. After 3nsec structure conformations are shows stable RMSD between 2.2Å – 2.7Å (Highlighted in red line) in 4 to 13nsec simulation time. After 13nsec RMSD shows some conformations changes due to second loop region 173-179 in protein and RMSD decrease 2.7Å to 1.6Åfor 2 nsec (13-14nsec). After 15nsec RMSD remain constant and stable between 1.4Å – 1.6Åto till end of the simulation time (Highlighted in red line).

Fluctuations in IDS3 protein residues were analyzed by backbone atoms motions and local changes in secondary structure elements. RMSF plot Fig. 6C shows acceptable fluctuations under 2.4Å with compare to beta factor (0.5Å – 0.8Å) aspect one large fluctuations higher than 3Å between 173 – 179 residues range. This range comes in loop region of protein that's why this region fluctuated during 13-14nsec simulation. Total 31.57% protein contributed in secondary structure (alpha helices=19.52% and beta strands =12.05%). SSE elements confirms that protein structure have stable conformations state aspect small loop (residues 173-179) that shows conformational changes during simulation. Based on acceptable RMSD around 1.5Å – 2.7Å and fluctuations between 1.0Å – 2.4Å confirms that protein has stable state during whole simulation time.

Discussion

In the present study, we reported that*Ids3* gene, which encodes a dioxygenase that converts DMA to MA or MA to epiHMA, is present in hexaploid wheat. These results are

contrary to a number of earlier reports showing absence of the *Ids3* gene(s) or presence of a mere pseudo gene in hexaploid wheat and its wild relatives (Nakanishi et al. 2000; Mori et al. 1990; Ma and Nomoto 1994) The bioinformatics analysis indicated that the functional wheat ortholog of *Ids3* gene might be present at chromosome 7AS, which is supported by the results obtained from physical mapping of the wheat ortholog in the telomeric region of chromosome 7AS. In the constructed phylogenetic tree, the close evolutionary relationship of *TaIds3_7AS* with *HvIds3* also supports the above results (Fig. 1). Our results are also supported by the location of most of the QTLs of high grain iron and zinc contents on chromosome 7A of different *Triticum* species (Tiwari et al. 2009; Peleg et al. 2009).The *Ids3* gene has been mapped on long arm of chromosome 4H of barley and long arm of chromosome 5R of rye using wheat-barley addition lines and wheat-rye addition lines respectively (Ma and Nomoto 1994; Mori and Nishizawa 1989; Ma et al. 1999).

The results of real-time RT-PCR showed the expression of wheat ortholog of *Ids3* gene in hexaploid wheat, which is strongly up-regulated under conditions of Fe-deficiency. According to the previous studies, during15-days of Fe starvation, the expression of *Ids3* was induced after three days of Fe-starvation in barley, which was gradually increased to a maximum level on the seventh day while the expression of *Ids3* gene was not observed in hexaploid wheat (Nakanishi et al. 2000). However, our results showed that the detectable expression of *Ids3* was observed five days after Fe-starvation and increased up to 15 days and thereafter its expression declined. So, the *Ids3* expression seemed to be more sensitive to Fe-deficiency in barley than in wheat. Similar expression pattern was reported for *Ids2* gene in barley. The *Ids2* expression in barley was hardly detectable at least for the first 7-days after the start of Fe-starved treatment (Okumura et al. 1994), while the expression of its ortholog in tobacco was clearly detectable within 3 days after Fe-starved treatment (Kobayashi et al., 2007). The induction of *Ids3* in barley is dependent on the availability of Fe and it is negatively correlated with the induction of NAS, NAAT and IDS3 enzymes and subsequently with secretion of MAs (Kobayashi and Nishizawa 2012; Higuchi et al. 1996; Kanazawa et al. 1998).These results strongly support the results of present investigation that the deficiency of Fe directly regulates the induction of *Ids3* expression in the roots of hexaploid wheat. Nakanishi et al. (1993) reported that the *Ids3* gene and its product detected only in Fe-deficient barley roots. Tolay et al. (2001) reported that as compared with diploid wheat (AA) and tetraploid wheat (AABB) species release higher amount of phytosiderophores under Fe deficiency. However, in case of Zn deficiency, diploid wheat species release higher amount of phytosiderophores than tetraploid wheat species. But in both the cases of deficiency,

hexaploid wheat was found to secrete highest amount of phytosiderophores than diploid and tetraploid wheat species.This might be because the genes responsible for synthesis of phytosiderophores are expressed predominantly and effectively when three genomes are present together.On the basis of "Draft genome of the wheat A-genome progenitor "*Triticum urartu*" (Ling et al. 2013), homology analysis of the *Hordeum vulgare* IDS3 protein as a query with BLASTp exhibited 65% identity with *Triticum urartu* (Accession no. EMS 480341) and predicts the molecular function exactly similar as HvIDS3 protein i.e.dioxygenase and oxidoreductase activity (http://www.uniprot.org/uniprot/M7ZIY2). These results suggest the presence of IDS3 protein ortholog also in diploid wheat, which might be responsible for higher secretion of phytosiderophores in Fe and Zn deficient conditions. The good correlation between the protein and RNA data demonstrates that regulation of gene expression by concentration of Fe is at the level of transcription or RNA stability and not at the level of translation, as in the case of Fe-regulated genes in other systems. In spite of the presence of *Ids3* gene and its mRNA transcripts in hexaploid wheat genome, the less RNA stability might be the reason to produce the optimum amount of IDS3 peptide to be detectable in the root exudates.

In the present study, the *HvIds3* gene sequence was aligned against wheat survey sequence. BLASTn results showed 74% sequence similarity with IWGSC_chr7AS_ab_k71_contigs of chromosome 7AS in wheat genome having same conserved domain. Results indicate the presence of putative ortholog of *HvIds3* in the short arm of chromosome 7A of hexaploid wheat genome. Further, results of structural alignment of proteins between *HvIds3* and *TaIds3*ortholog by FATCAT server showing 57.25% similarity of *HvIds3* with putative wheat ortholog of *Ids3* indicated significant structural similarity in the proteins of both the genes which is an agreement with the observations of (Domingues et al. 2000). According to Domingues et al. (2000), if a protein has more than 40% sequence identity to another protein whose biochemical function is known and if the functionally important residue (for example, those in the active site of an enzyme) are conserved between the two protein, a reasonable working assumption can be made that the two proteins have a similar biochemical function. ProFunc analysis also identified the functional motifs of TaIDS3 and showed the close relationships of TaIDS3 to functionally characterized HvIDS3 protein. Even the subcellular locations of the gene in both wheat and barley was found in cytoplasm also suggests the presence of putative barley ortholog in wheat. Crystal structure of cereals IDS3 protein is not available in PDB yet. Moreover, high-throughput protein structure methods, such as yeast X-ray crystallography and NMR, cannot be easily applied to due to their high cost. Therefore,

homology modeling for predicting RWP-RKs protein structure and function could provide alternative solutions. Homology modeling referred to as comparative or knowledge based modeling method, rely on detectable significant similarity between the query amino acid sequences and protein of know 3D structure (resolved by X-ray crystallography and NMR) and can be used to modelled the 3D structure of all the members of a protein family using a single representative 3D structure as an initiating point (Kumar et al. 2013; Kumar et al. 2016).The TaIDS3 sequence alignment with template is needed because Swiss-Model algorithm can discover structural information based on sequence. This alignment information is applied to simulation of target structure. Sequence alignment quality of target and template is important to predict a good homology model. Swiss-Model algorithm was predicted the 3D structure of TaIDS3 with good stero-chemical properties.

After protein structure modeling of ids3, we go for stability and local changes in structure analysis through molecular dynamics (MD) simulation for small time scale. Ids3 predicted model was place into cytoplasmic condition under TIP3P water molecules (Fig 6A). MD results suggest that predicted Ids3 protein model have stable state during simulation between 1.4Å – 2.7Åaverage rmsd (Fig. 6B). Root mean square fluctuations value between 1.4Å -2.4Å shows stable fluctuations in protein that compatible with experimental beta factor (Fig5C). One large fluctuation in TYR177 residues that comes in loop region is reported between 3.2Å-5.7ÅRMSF. This large fluctuation doesn't affect the local changes in secondary structure conformations. The percentage of secondary structure elements (31%) also shows that predicted model have stable conformation during simulation (Fig 6D).

Conclusions

The present study first time reported the *HvIds3* ortholog in the hexaploid wheat genome and physically mapped on telomeric region of chromosome 7AS. The expression analysis reflected that Fe deficiency directly regulates the induction of *Ids3* gene in Chinese Spring roots. Modeling and MD simulations results of HvIDS3 revealed that identified IDS3 is stable at cell during Fee deficiency. Identified *TaIDS3* being utilizing by us in ongoing marker assisted program (MAS) to develop the Fe efficient wheat cultivar and boost up the biofortification program. However, extensive characterization and functional validation of *IDS3* gene in other cereals is also necessary to further explore their biological roles using different reverse genetics approaches like RNAi and VIGS.

Author's Contribution

SK and HSD designed and supervised the study. PM, UK and AK designed experiment and analyzed the data as a whole and wrote the manuscript. SM and PM collected samples for the analysis. AK and SK performed the molecular dynamics analysis. All authors read and approved the final manuscript.

Acknowledgement

Thanks to Dr. B. S. Gill for providing the cytogenetic stocks for mapping.

Conflict of interest

The authors declare that they have no conflict of interest.

References

Cakmak I (2008) Enrichment of cereal grain with zinc: agronomic or genetic Biofortification? Plant Soil 302:1-17

Domingues FS, Lackner P, Andreeva A, Sippl MJ (2000) Structure based evaluation of sequence comparison and fold recognition alignment accuracy. J Mol Biol 297:1003-1013

Endo TR, Gill BS (1996) The deletion stock of common wheat. J Hered 87:295-307

Higuchi K, Kanazawa K, Nishizawa NK, Mori S (1996) The role of nicotianamine synthase in response to Fe nutrition status in Gramineae. Plant and Soil 178:171-177

Kanazawa K, Higuchi K, Nakanishi H, Nishizawa NK, Mori S (1998) Characterizing nicotianamine aminotransferase: improving its assay system and details of the regulation of its activity by Fe nutrition status. Soil Sci Plant Nutr 44:717-721

Kobayashi T, Nishizawa NK (2012) Iron uptake, translocation and regulation in higher plants. Annu Rev Plant Biol 63:131-52

Kobayashi T, Yoshihara T, Itai RN, Nakanishi H, Takahashi M, Mori S, Nishizawa NK (2007) Promoter analysis of iron-deficiency-inducible barley IDS3 gene in *Arabidopsis* and tobacco plants. Plant Physiol Biochem 45:262-269

Ling HQ, Zhao S, Liu D, Wang J, Sun H et al. (2013) Draft genome of the wheat A-genome progenitor *Triticum urartu*. Nature 496: 87-90

Livak KJ, Schmittgen TD (2001) Analysis of relative gene expression data using real-time quantitative PCR and the $2^{-\Delta\Delta C}$T method. Methods 25: 402-408

Ma JF, Nomoto K (1993) Two related biosynthetic pathway of mugineic acids in gramineous plants. Plant Physiol 102:373-378

Ma JF, Nomoto K (1994) Incorporation of label form ^{13}C-, ^{2}H-and ^{15}N-labeled methionine molecules during the biosynthesis of 2'-deoxymugineic acid in roots of wheat. Plant Physiol 105:607-610

Ma JF, Taketa S, Chang YC, Takeda K, Matsumoto H (1999) Biosynthesis of phytosiderophores in several Triticeae species with different genomes. J Exp Bot 50:723-726

456 Maroof MA, Biyashev RM, Yang GP, Zhang Q, Allard RW (1994) Extraordinarily
457 polymorphic microsatellite DNA in barley: species diversity, chromosomal locations and
458 population dynamics. Pro Natl Acad Sci 91:5466-5470
459
460 Mori S, Nishizawa N (1989) Identification of barley chromosome no. 4 possible encoder of
461 genes of mugineic acid synthesis from 2-deoxymugineic acid using wheat-barley addition
462 lines. Plant Cell Physiol 30:1057
463
464 Mori S, Nishizawa N, Fujigaki J (1990) Identification of rye chromosome 5R as a carrier of
465 the genes for mugineic acid synthetase and 3-hydroxymugineic acid synthetase using wheat-
466 rye addition lines. Jpn J Genet 65:343-352
467
468 Nakanishi H, Okumura N, Umehara Y, Nishizawa NK, Chino M, Mori S (1993) Expression
469 of a gene specific for iron deficiency (*Ids3*) in the roots of *Hordeum vulgare*. Plant Cell
470 Physiol 34:401-410
471
472 Nakanishi H, Yamaguchi H, Sasakuma T, Nishizawa NK, Mori S (2000) Two dioxygnase
473 genes, *Ids3* and *Ids2*, from *Hordeum vulgare* are involved in the biosynthesis of mugineic
474 acid family phytosiderophores. Plant Mol Biol 44:199-207
475
476 Neelam K, Rawat N, Tiwari VK, Tripathi SK, Randhawa GS, Dhaliwal HS (2011)
477 Evaluation and identification of wheat-*Aegilops* addition lines controlling high grain iron
478 and zinc content and mugineic acids production. Cereal Res Commun 40:53-61
479
480 Okumura N, Nishizawa NK, Umehara Y, Ohata T, Nakanishi H, Yamaguchi H, and Chino
481 M, Mori S (1994) A dioxygenase gene (*Ids2*) expressed under iron deficiency conditions in
482 the roots of *Hordeum vulgare*. Plant Mol Biol 25:705–719
483
484 Paolacci RA, Oronzo AT, Porceddu E, Ciaffi M (2009) Identification and validation of
485 reference genes for quantitative RT-PCR normalization in wheat. BMC Mol Bio 10:1-27
486
487 Peleg Z, Cakmak I, Ozturk L, Yazici A, Jun Y, Budak H, Korol AB, Fahima T, Saranga Y
488 (2009) Quantitative trait loci conferring grain mineral nutrient concentrations in durum wheat
489 X wild emmer wheat RIL population. Theor Appl Genet 119:353-369
490
491 Romheld V, Marschner H (1990) Genotypical differences among graminaceous species in
492 release of phytosiderophores and uptake of iron phytosiderophores. Plant Soil 123:147-153
493 Sears ER (1954) The aneuploids of common wheat. University Archives of the University of
494 Missouri-Columbia USA
495
496 Sears ER (1964) Nullisomic-tetrasomic combinations in hexaploid wheat. Chromosome
497 Manipulation and Plant Genetics 29-45
498
499 Sears ER, Sears LMS (1978, February) The telocentric chromosomes of common wheat. In
500 Proceedings of the 5th International wheat genetics symposium (Vol.1, pp. 389-407). Indian
501 Society of Genetics and Plant Breeding New Delhi
502
503 Singh K, Sasakuma T, Bughio N, Takahashi M, Nakanishi H, Yoshimura E, Nishizawa NK,
504 Mori S (2000) Ability of ancestral wheat species to secrete mugineic acid family
505 phytosiderophores in response to iron deficiency. J Plant Nutr 23: 1973-1981

Takagi S (1976) Naturally occurring iron-chelating compounds in oat- and rice- root washings I. Activity measurement and preliminary characterization. Soil Sci Plant Nutr 22:423-433

Takahashi M (2003) Overcoming Fe deficiency by a transgenic approach in rice. Plant Cell Tissue Organ Culture 72:211-220

Tegelstrom H (1992) Detection of mitochondrial DNA fragments. Molecular genetic analysis of populations: a practical approach. IRL Press, Oxford, 89-114

Tiwari VK, Rawat N, Chhuneja P, Neelam K, Aggarwal R, Randhawa GS, Dhaliwal HS, Keller B, Singh K (2009) Mapping of Quantitative trait loci for grain iron and zinc concentration in diploid A genome wheat. J Heredity 100:771-776

Tolay I, Erenoglu B, Romheld V, Braun HJ, Cakmak I (2001) Phytosiderophore release In *Aegilops tauschii* and *Triticum* species under zinc and iron deficiency. J Exp Bot 52(358):1093-1099

Treeby M, Marschner H, Romheld V (1989) Mobilization of iron and other micronutrient cations from calcareous soil by plant-borne, microbial, and synthetic metal chelators. Plant Soil 114:217-226

vonWiren N, Khodr H, Hider RC (2000) Hydroxylated phytosiderophore species possess an enhanced chelate stability and affinity for Iron(III). Plant Physiol 124:1149-1157

vonWiren N, Romheld V, Shioiri T, Marschner H (1995) Competition between microorganisms and roots of barley and sorghum for iron accumulated in the root apoplasm. New Phytol 130:511-521

Shivakumar D, Williams J, Wu Y, Damm W, Shelley J, Sherman W (2010) Prediction of absolute solvation free energies using molecular dynamics free energy perturbation and the OPLS force field. J Chem Theory Comput 6:1509–1519

Guo Z, Mohanty U, Noehre J, Sawyer TK, Sherman W, Krilov G (2010) Probing the α-helical structural stability of stapled p53 peptides: molecular dynamics simulations and analysis. Chem Biol Drug Des 75: 348-359

Bowers KJ, Chow E, Xu H, O. Dror R, Eastwood MP, Gregersen BA, Klepeis JL, Kolossvary I, Moraes MA, Sacerdoti FD, Salmon JK, Shan Y, Shaw DE (2006) Scalable Algorithms for Molecular Dynamics Simulations on Commodity Clusters. Proceedings of the ACM/IEEE Conference on Supercomputing (SC06), Tampa, Florida, November 11-17

Schrödinger Release 2017-2: Desmond Molecular Dynamics System, D. E. Shaw Research, New York, NY, 2017

Maestro-Desmond Interoperability Tools, Schrödinger, New York, NY, 2017

Jorgensen WL, Maxwell DS, Tirado-Rives J (1996) Development and testing of the OPLS all-atomforce field on conformational energetics and properties of organic liquids. J Am Chem Soc 118: 11225

552 Kaminski G, Friesner RA, Tirado-Rives J, Jorgensen WL (2001) Evaluation and
553 reparameterization of the OPLS-AA force field for proteins via comparison with accurate
554 quantum chemical calculations on peptides. J Phys Chem B 105: 6474–6487

555 Jorgensen WL, Chandrasekhar J, Madura JD, Impey RW, Klein ML (1983) Comparison of
556 simple potential functions for simulating liquid water. J Chem Phys 79: 926–935

557 Hui Li, Robertson AD, Jensen JH (2005) Very fast empirical prediction and interpretation of
558 protein pKa values. Proteins 61: 704-721

559 Nosé, S (1984) A unified formulation of the constant temperature molecular-dynamics
560 methods. J Chem Phys 81: 511–519

561 Hoover WG (1985) Canonical dynamics: Equilibrium phase-space distributions. Phys Rev A
562 31: 1695–1697

563 Martyna GJ, Tobias DJ, Klein ML (1994) Constant pressure molecular dynamics algorithms.
564 J Chem Phys. 101: 4177-4189

565

566

567

568

569

570

571

572

573

574

575

576

577

578

579

580

581 **Tables:**

582 **Table 1. Primers used for chromosomal location of *TaIds3*.**

583
584 **Table 2. Primers for relative expression analysis of *TaIds3*.**
585

586 Table 1.

Name	Primer Sequences (5′-3′)
TaIds3 7AS F	TTGGTTACGACCTGCAAGAAA
TaIds3 7AS R	ACCATTACCCAAGGTGCTCG

587

588 Table 2.

Name	Primer Sequences (5′-3′)	Application
*Ids3*cDNAF	CGTCGGCGACACCAAGA	For real-time RT-PCR for *Ta Ids3*
*Ids3*cDNA R	CACCTCGCGGAGCTTTTG	
ADP rf F	GGGTTGTACGAGGGTCTTGA	Housekeeping gene for Real-time –RT PCR
ADP rf R	TCCAGCACGTTTGTTTCTTG	

589

590 **Figures:**

591 **Fig.1 (A)** TaIDS gene structure; (**B**) representation of functional domains and their respective
592 superfamiles; (**C**) interactive ribbon view and surface representation of TaIDS3 protein:
593 Right: view from back of molecule via vertical rotation by 180°. Figure was prepared using
594 UCSF-Chimera.

595
596 **Fig 2 Neighbour-joining phylogenetic tree of the *Ids3* and *Ids2* members;** The tree was
597 constructed with the amino acid sequences of *Ids3* and *Ids2* proteins from Barley (Hv), Rice
598 (Os) and Wheat (Ta) using the neighbour-joining method in MEGA 6.0 software. A bootstrap
599 with 1000 repetitions was included.
600
601 **Fig.3** Polyacrylamide gel electrophoresis analysis of the PCR products of *TaIds3* amplified
602 using nullisomic-tetrasomic and ditelosomic lines of *T. aestivum* cv. Chinese Spring.
603
604 **Fig.4 Physical map of Chinese Spring chromosome 7A;** The identification of deletion line
605 fraction arm length (FL) values breakpoints is indicated on the right in parentheses. The
606 telomeric bin of 7AS shows the putative location of the *TaIds3* gene.
607

Fig.5 Relative expression level (change in fold) of *TaIds3* gene in roots of *T. aestivum* cv. Chinese Spring;Under Fe-sufficient and -deficient conditions at 5, 10, 15, 25 and 35 days after transplantation of seedlings in hydroponic condition. The means of three independent experiments are shown. Error bars indicate Standard Deviation.

Fig. 6 Molecular dynamics simulation results of HvIDS3 protein model. A. Simulation box with TIP3P water model, **B.** RMSD plot of IDS3 backbone atoms, **C.** RMSF plot with beta factor (experimental x-ray B-factor) of IDS3 backbone atoms and **D.** secondary structure elements of IDS3 protein model during simulation.

Figure 1.

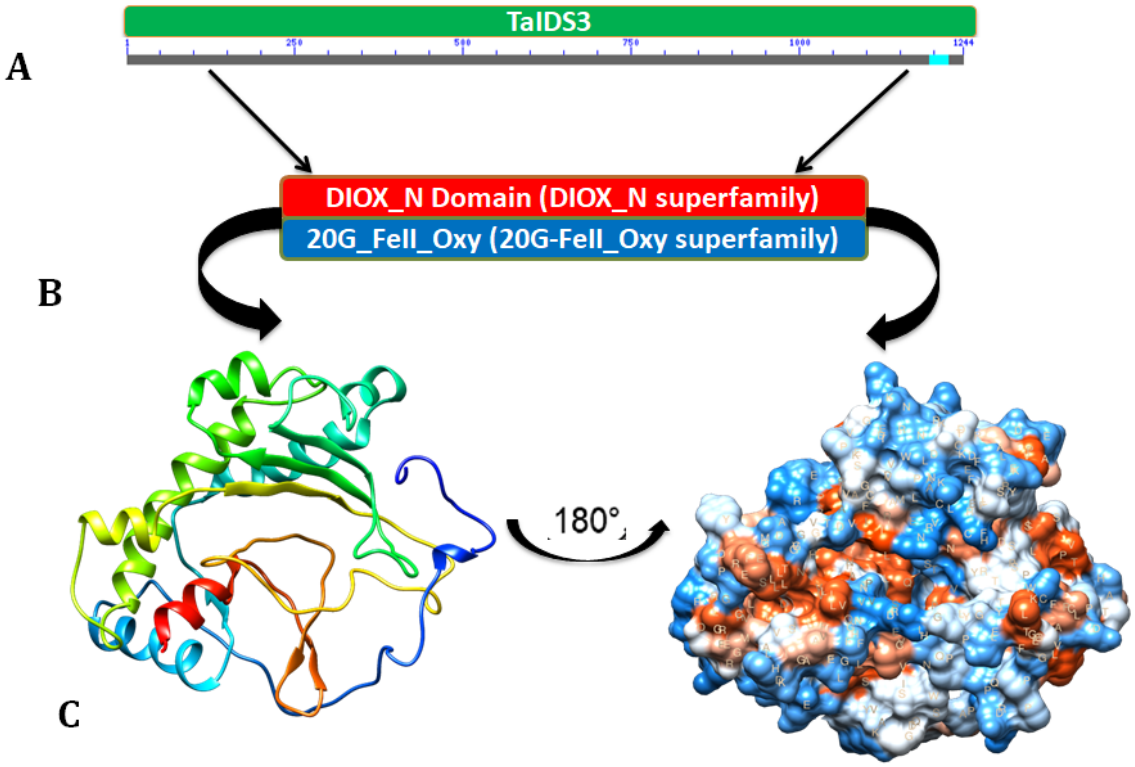

Figure 2.

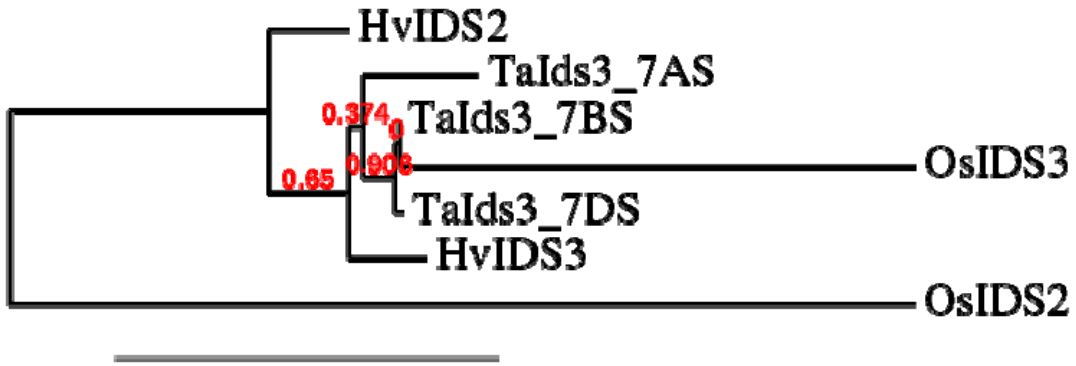

624

625

626 **Figure 3.**

627

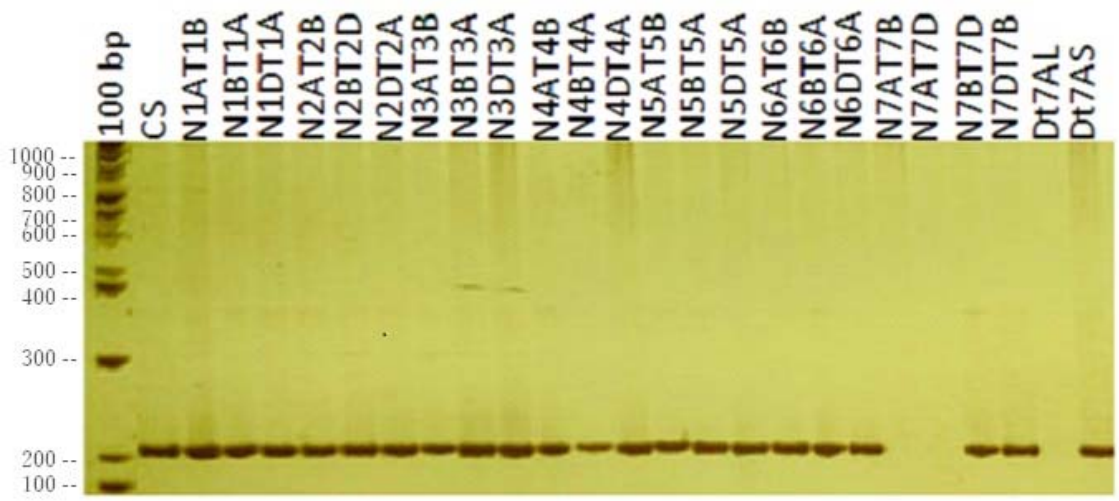

628

629

630 **Figure 4.**

631

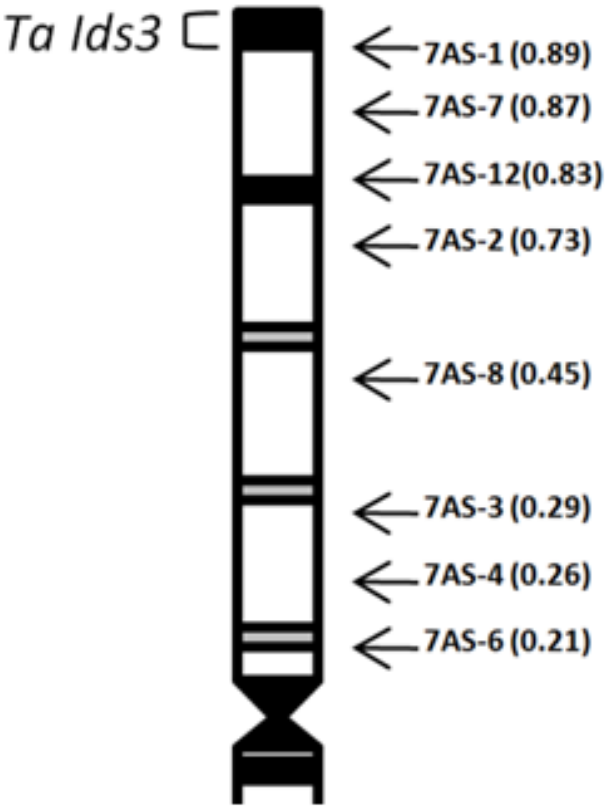

Figure 5.

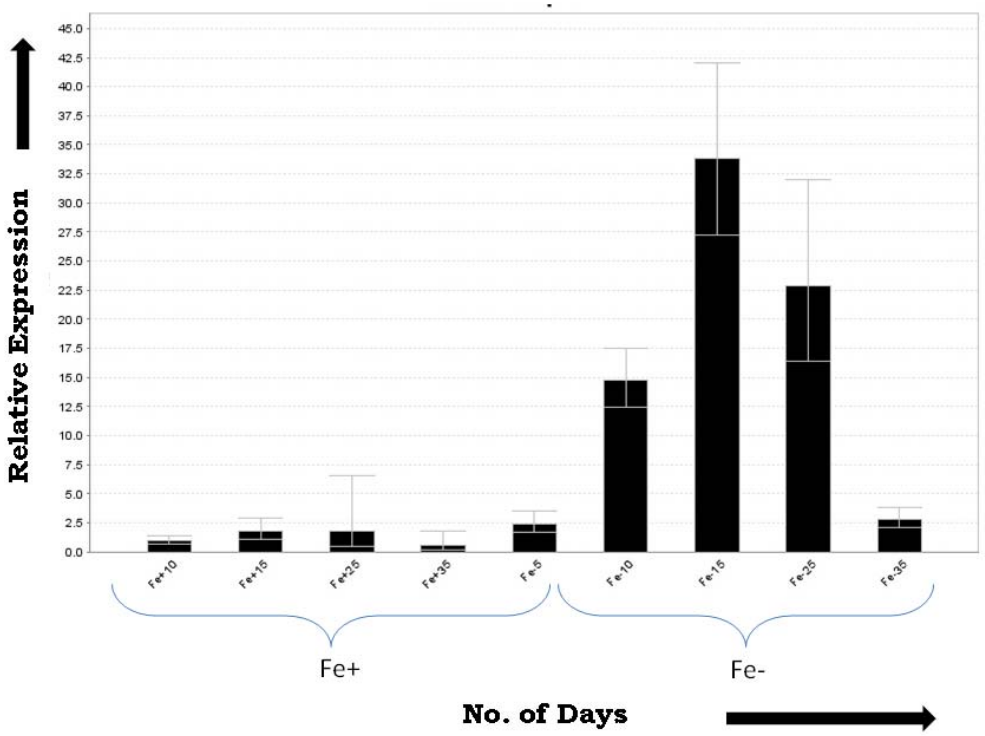

636

637 **Figure 6.**

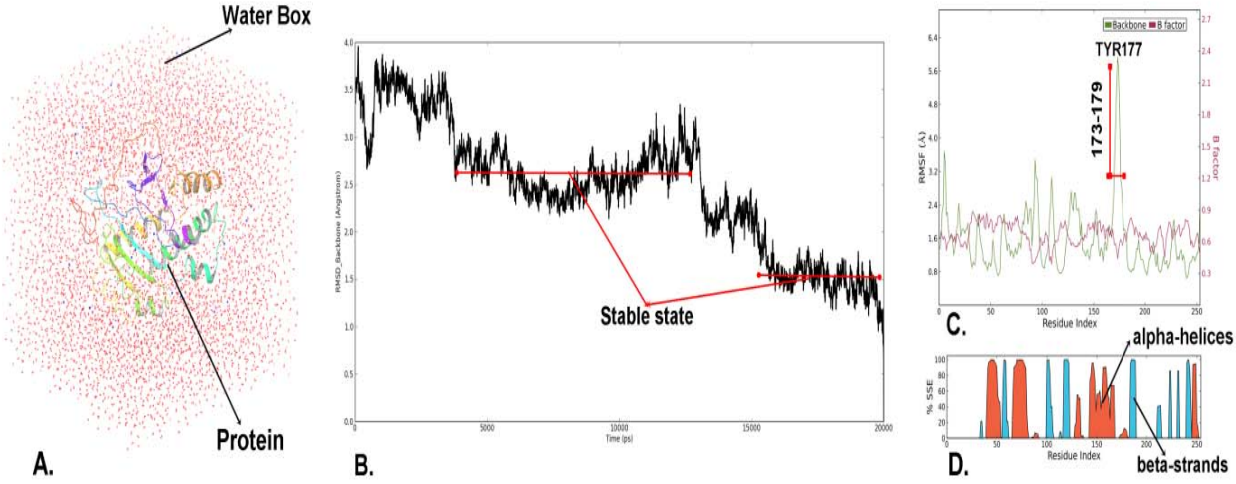

638

639

640

641

642

643

644

645